

BlitzGS: City-Scale Gaussian Splatting at Lightning Speed

ZHONGTAO WANG[†] HUIZHAN AU[†] YILONG LI MAI SU HAOJIE JIN
YISONG CHEN^{*} MENG GAI FEI ZHU^{*} GUOPING WANG

Peking University, China

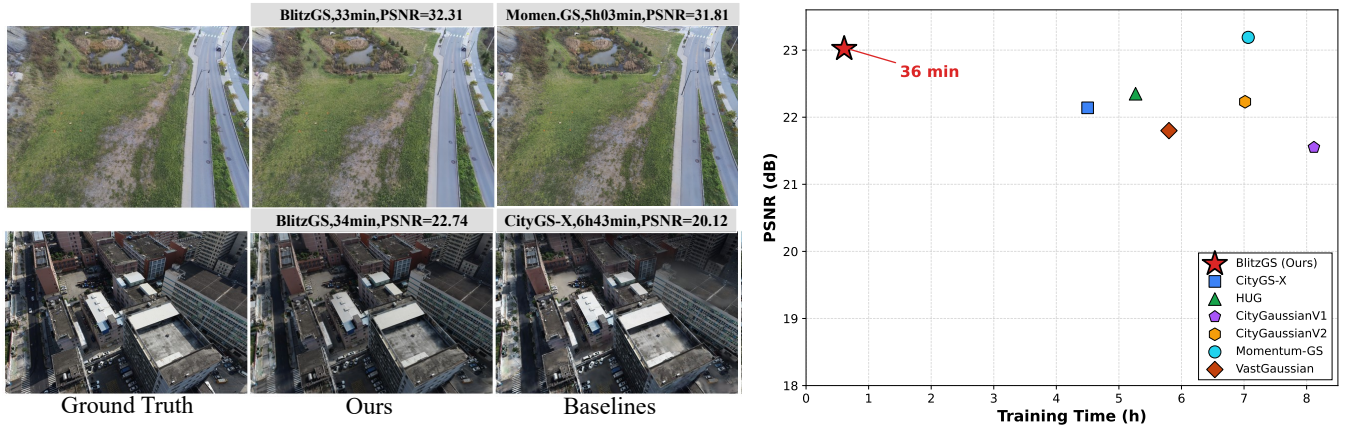


Figure 1. **Left:** Qualitative comparison on *Rubble* (top) and *Residence* (bottom): ground truth, BlitzGS, and a representative large-scale baselines. **Right:** Training time vs. PSNR on *Building* (4x A6000 GPUs). BlitzGS trains in under an hour while maintaining high quality.

Large-scale 3D Gaussian Splatting underpins applications in digital twins, simulation, and aerial mapping; however, city-scale training remains computationally expensive. Training remains slow despite multi-GPU execution because every iteration must preprocess, communicate, and rasterize an overly dense set of primitives. At any given step, only a small fraction of these primitives contribute meaningfully to the loss; the rest incur redundant storage, communication, and rasterization costs without contributing to model convergence. Existing approaches improve these individual cost factors, yet they do not fully address the underlying workload question: *which Gaussians should be stored on each GPU, rendered for each view, and retained after early geometry formation?*

We present **BlitzGS**, a distributed 3DGS framework that reduces active Gaussian workload for fast city-scale reconstruction. BlitzGS manages this workload at three coupled levels. At the system level, the framework shards Gaussians across GPUs by index parity rather than spatial blocks. This approach mitigates the cross-block visibility redundancy inherent in spatial partitioning. Furthermore, it distributes each rendering step through a single cross-GPU exchange that routes projected Gaussians to their tile owners. At the model level, scheduled importance-scoring passes shrink the global Gaussian population. During these passes, the framework generates a per-Gaussian visibility weight to bias density-control updates toward contributing primitives and a per-view importance mask for the view-level renderer. At the view level, BlitzGS trims each camera’s active set with a distance-based LOD gate to exclude excessively fine primitives for the current frustum and the importance-based culling mask to skip Gaussians with negligible cross-view contribution.

On large-scale benchmarks, BlitzGS matches the rendering quality of recent large-scale baselines while delivering an order-of-magnitude speedup, training city-scale scenes in tens of minutes. Our code is available at <https://github.com/AkierRae/BlitzGS>.

CCS Concepts: • **Computing methodologies** → **Image-based rendering; Rendering.**

[†]Equal contribution. ^{*}Corresponding author.

Additional Key Words and Phrases: 3D Gaussian Splatting, Large-Scale Reconstruction

1 Introduction

City-scale 3D reconstruction has become a foundation for applications such as aerial survey inspection, digital twins, and simulation assets. These applications often begin with thousands of calibrated images, and they require more than eventual high-quality novel views. A city-scale reconstruction system in practice needs to build a scene quickly, use multiple GPUs efficiently, and render robustly across a wide range of viewing distances. While 3DGS works well on small scenes, it becomes much less effective in large-scale reconstruction. The vanilla pipeline becomes too slow to be practical, and the resulting model often struggles to preserve distant structures and large spatial extents.

Recent large-scale 3DGS work has addressed this cost from several directions, including distributed training [Chen and Lee 2024; Gao et al. 2025], hierarchical scene partitioning with LOD rendering [Kerbl et al. 2024; Liu et al. 2024; Ren et al. 2024], and partition-and-merge scaling [Lin et al. 2024; Liu et al. 2024; Su et al. 2025]. Even with these advances, city-scale optimization remains expensive, typically spanning several hours across multi-GPU nodes. Training time remains a major bottleneck, and existing methods still trade off scene quality for training speed.

These methods each accelerate a different part of the pipeline, but they share a common inefficiency. In any single iteration of city-scale 3DGS training, only a small fraction of the Gaussians contribute to the rendered loss, while the rest still incur the full cost of training. Some sit on a different GPU from the tile being rendered and must be communicated across devices before they can contribute. Others are too fine for the current camera and pass

through projection and rasterization without affecting any pixel. The rest are redundant clones introduced by densification that never become distinct from their parents. The dominant cost of city-scale 3DGS is therefore not only the absolute size of the Gaussian set, but the share of *wasted work* performed on Gaussians that should not have been touched in the current step.

Our observation is that fast city-scale reconstruction should minimise the number of Gaussians that enter the rendering pipeline. Globally, the model should remove redundant clone-and-split leftovers after densification so they do not survive into the rest of the training. Locally, each view should activate only the scales that are useful for its camera distance, so distant or sub-pixel Gaussians do not incur unnecessary rasterization cost. Doing this at city scale requires a carefully designed importance signal: aerial captures have very uneven view overlap, with valid roofs, facades, and scene boundaries often seen by only a few grazing cameras and easily confused with redundancies.

We present **BlitzGS**, a distributed 3DGS framework that reduces the active Gaussian workload for fast city-scale reconstruction. BlitzGS controls this workload at three coupled levels. At the *system level*, it shards Gaussians across GPUs by index parity rather than by spatial blocks, so each device holds a balanced scene-wide slice and avoids the cross-block visibility waste that spatial partitioning incurs. Each render step is then distributed across the same GPUs through a single cross-GPU exchange that routes projected Gaussians to their tile owners, spreading per-step projection and rasterization. At the *model level*, scheduled importance-scoring passes shrink the global population while emitting, in the same sweep, a per-Gaussian multi-view visibility weight that biases density-control updates toward consistently contributing primitives and a per-view importance mask consumed by the view level renderer. At the *view level*, BlitzGS trims each camera’s active set with two complementary mechanisms: a distance-based LOD gate that drops Gaussians too fine for the current camera, and the importance-based culling mask that additionally skips Gaussians with negligible cross-view contribution. The three levels therefore reduce the overall cost in different ways: per-GPU load, global model size, and per-view active set, so the same iteration touches fewer primitives at every stage of training.

Across Mill-19, UrbanScene3D, and *MatrixCity*, BlitzGS matches the rendering quality of recent large-scale baselines while training city-scale scenes in tens of minutes on four A6000 GPUs. As shown in Figure 1, this yields an order-of-magnitude training speedup, attributable to the workload reductions delivered by the three-level pipeline design. Ablation studies confirm that each level contributes to the final speed-quality trade-off.

In summary, our contributions are threefold:

- **Insight.** A unifying workload-centric view of city-scale 3DGS acceleration: we design every component around one principle—each operation should touch only the Gaussians that matter at the corresponding device, view, and training stage.
- **Method.** We propose a fast distributed reconstruction framework that reduces workload at three coupled levels: system level sharding with distributed rendering, model level simplification

feeding back into density control, and view level filtering by LOD and importance.

- **Experiment.** On large-scale benchmarks, BlitzGS achieves order-of-magnitude faster training while maintaining rendering quality comparable to recent city-scale 3DGS baselines.

2 Related Work

2.1 3D Gaussian Splatting

3D Gaussian Splatting (3DGS) [Kerbl et al. 2023] represents scenes with explicit anisotropic Gaussian primitives and differentiable tile-based rasterization, achieving real-time rendering quality competitive with neural radiance fields [Barron et al. 2022; Fridovich-Keil et al. 2022; Mildenhall et al. 2021; Müller et al. 2022]. Its efficiency comes from avoiding per-ray MLP queries, but training still depends on progressive densification, where a growing Gaussian set is repeatedly cloned, split, pruned, and optimized over tens of thousands of iterations. Many works improve this representation from complementary directions. Scaffold-GS [Lu et al. 2024] and Octree-GS [Ren et al. 2024] introduce structured anchor or LOD representations; Mip-Splatting [Yu et al. 2024a] improves anti-aliasing; AbsGS [Ye et al. 2024], Pixel-GS [Zhang et al. 2024], Gaussian-Pro [Cheng et al. 2024], 3DGS-MCMC [Kheradmand et al. 2024], and Revising-3DGS [Rota Bulò et al. 2024] refine densification or optimization; 2DGS [Huang et al. 2024], PGSR [Chen et al. 2024a], SuGaR [Guédon and Lepetit 2024], and Gaussian Opacity Fields [Yu et al. 2024b] improve geometric fidelity; and Compact-3DGS [Li et al. 2023b], LightGaussian [Fan et al. 2024b], and MaskGaussian [Liu et al. 2025b] reduce storage through compression or pruning. These advances improve quality, geometry, or compactness, while BlitzGS focuses on the training workload itself: how many Gaussians are stored, rendered, communicated, and updated during city-scale optimization.

2.2 Large-Scale Scene Reconstruction

Scaling neural scene reconstruction to city-scale captures is commonly handled by decomposition. NeRF-based systems such as Block-NeRF [Tancik et al. 2022], Mega-NeRF [Turki et al. 2022], and Switch-NeRF [Zhenxing and Xu 2022] partition scenes or route samples to local models. 3DGS methods follow related directions: VastGaussian [Lin et al. 2024] trains large aerial scenes through progressive data partitioning; CityGaussianV1 [Liu et al. 2024] combines block-wise reconstruction with LOD rendering; CityGaussianV2 [Liu et al. 2025a] improves geometric reconstruction and compression; HUG [Su et al. 2025] uses visibility-based partitioning with hierarchical urban Gaussians; GigaGS [Chen et al. 2024b], LetsGo [Cui et al. 2024], and RetinaGS [Li et al. 2024] further explore high-resolution, LiDAR-assisted, or foveated large-scene settings. Hierarchy-GS [Kerbl et al. 2024] builds a multi-scale Gaussian hierarchy for large datasets, DOGS [Chen and Lee 2024] uses distributed optimization with ADMM-style Gaussian consensus. These block-based pipelines make training easier, but they must manage block overlap, boundary consistency, and final rendering across separately optimized parts. Distributed large-scale methods reduce this bottleneck more directly. Momentum-GS [Fan et al. 2025] improves

block consistency through momentum self-distillation, and CityGS-X [Gao et al. 2025] avoids the partition-and-merge paradigm with a parallel hybrid hierarchical representation and batch-level multi-task rendering. These systems make large reconstruction more scalable or more geometrically accurate. BlitzGS targets a different goal: minute-level city-scale reconstruction by reducing the Gaussian workload per device, per view, and throughout training.

2.3 Efficient Gaussian Splatting Optimization

Accelerating 3DGS optimization has become an important direction. Mini-Splatting [Fang and Wang 2024] and Mini-Splatting2 [Fang and Wang 2025] speed up small-scene training through densification and simplification strategies; Taming 3DGS [Mallick et al. 2024] studies selective pruning and steerable importance; InstantSplat [Fan et al. 2024a] accelerates small-scene reconstruction with feed-forward initialisation; Scaling 3DGS [Zhao et al. 2025] explores distributed system support for larger Gaussian workloads; and large-batch analyses [Yao et al. 2018] provide useful context for batch-level optimization. FastGS [Ren et al. 2025] further redesigns adaptive density control around multi-view consistent densification and pruning, and uses a compact box to reduce unnecessary Gaussian-tile pairs, enabling around 100-second training on standard small-scene benchmarks. Its emphasis on strict Gaussian-count control is closely related to our workload view, while BlitzGS extends this principle to distributed city-scale training, where per-device ownership, per-view activation, and contribution-guided global simplification jointly drive the speedup. Complementary systems work improves the renderer itself: FlashGS [Feng et al. 2025] accelerates rasterization through memory reuse, DISTWAR [Durvasula et al. 2023] improves gradient-pass atomic operations, and StopThePop [Radl et al. 2024] addresses popping artefacts from depth sorting. Most optimization-oriented methods are designed for small scenes or kernel-level acceleration, while large-scale systems still spend substantial work on dense active Gaussian sets. BlitzGS makes workload reduction the primary acceleration mechanism in the city-scale setting, combining distributed primitive ownership, view level activation, and contribution-guided multi-view simplification so that fewer Gaussians enter the expensive parts of training.

3 Method

Given posed aerial images $\{I_v\}_{v=1}^V$ and an SfM point cloud, BlitzGS reconstructs an explicit 3DGS model under distributed training. Each Gaussian remains a standard primitive with position, covariance, opacity, and SH color. The method follows a single rule: **a city-scale optimization should avoid touching Gaussians that are unnecessary for the current device, view, or training stage**. As shown in Figure 2, we instantiate this rule at three coupled levels: system level sharding with distributed rendering, model level simplification that feeds an importance signal back to density control and view filtering, and view level trimming by LOD and importance.

3.1 Preliminaries

3DGS [Kerbl et al. 2023] represents a scene with a set of explicit anisotropic primitives $\mathcal{G} = \{g_i\}_{i=1}^N$. Each Gaussian stores a center μ_i , a covariance Σ_i , an opacity α_i , and view-dependent color $\mathbf{c}_i(\mathbf{d})$

parameterised by spherical harmonics:

$$G_i(\mathbf{x}) = \exp\left(-\frac{1}{2}(\mathbf{x} - \mu_i)^\top \Sigma_i^{-1}(\mathbf{x} - \mu_i)\right). \quad (1)$$

Following the standard 3DGS parameterization, the covariance is represented by learnable rotation and scale components.

For a camera view, Gaussians are projected to screen-space ellipses and rasterized by tile-based front-to-back alpha compositing. For pixel \mathbf{p} , the rendered color is

$$\hat{\mathbf{C}}(\mathbf{p}) = \sum_{i \in \mathcal{N}(\mathbf{p})} T_i(\mathbf{p}) \alpha_i G'_i(\mathbf{p}) \mathbf{c}_i(\mathbf{d}), \quad T_i(\mathbf{p}) = \prod_{j < i} (1 - \alpha_j G'_j(\mathbf{p})), \quad (2)$$

where $\mathcal{N}(\mathbf{p})$ denotes the depth-ordered projected Gaussians overlapping the pixel, G'_i is the projected 2D Gaussian value, and T_i is accumulated transmittance. Training optimizes these primitive attributes from posed images and an initial point cloud, while adaptive density control periodically clones, splits, and prunes Gaussians. In city-scale reconstruction, the dominant cost is therefore not only the number of images, but also the number of active Gaussians that must be projected, exchanged across devices, rasterized, and updated at every iteration. BlitzGS is designed around reducing this active workload at the system, view, and model levels.

3.2 System Level Primitive Sharding

A city-scale model contains hundreds of millions of Gaussian primitives, far more than a single GPU can store and optimize. Spatial block partitioning sidesteps this limit but pays for it with cross-block visibility waste, imbalanced shards, and a final merge step. BlitzGS avoids these costs at the system level by sharding the global Gaussian model across M GPUs by index parity rather than by world-space region, and by distributing each render step across the same GPUs. Both storage and per-step compute therefore scale with the GPU count.

Each GPU stores only its local shard $\mathcal{G}^{(m)}$ (approximately $|\mathcal{G}|/M$ Gaussians) and its optimizer state. At each rendering iteration, every GPU projects only its own local Gaussians. The image being rendered is partitioned into tiles, each assigned to one GPU. After projection, every GPU exchanges its projected Gaussians with every other GPU in a single all-to-all step. Each Gaussian is routed to whichever GPUs own the tiles it lands on, and each GPU then composites the pixels of its tiles from the Gaussians it received. Both projection and rasterization are therefore distributed every step, while the rendered image stays identical to what a single-GPU renderer would produce on the same Gaussian set. This scheme is more compact than block partition (Figure 3), where a block-bound GPU has to process Gaussian beyond its region whenever a camera straddles a boundary, so the savings shrink as more cameras straddle.

Two automatic load-balancing mechanisms keep this distribution productive. After density control changes the population, an index-parity redistribution rebalances shard sizes across GPUs once the per-GPU skew exceeds a fixed threshold. Within each iteration, a cost-aware tile partition [Zhao et al. 2025] keeps rasterization load balanced across GPUs.

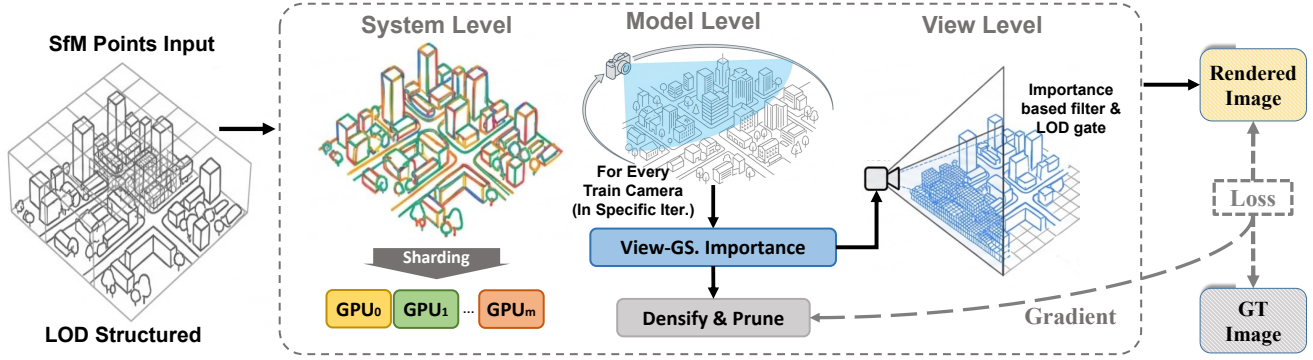


Figure 2. **Pipeline of BlitzGS.** The SfM cloud is voxelised at multiple scales and each Gaussian inherits an LOD level. The three levels of active workload control then cut per-iteration cost at different scopes. The *system level* shards Gaussians across M GPUs non-spatially, so each rank’s slice spans the whole scene rather than a world-space region; the rendering itself is also distributed across all ranks. The *model level* interleaves scheduled simplification with density control: each importance-scoring pass shrinks the global population and emits a per-(Gaussian, camera) importance signal that reweights density-control gradients so the smaller model concentrates the remaining densification on consistently-contributory primitives, and that also feeds the view level filter. The *view level* trims each camera’s active set with a distance-based LOD gate plus an importance-driven cull. Training is supervised by an L1+SSIM photometric term combined with a scale regulariser on visible Gaussians.

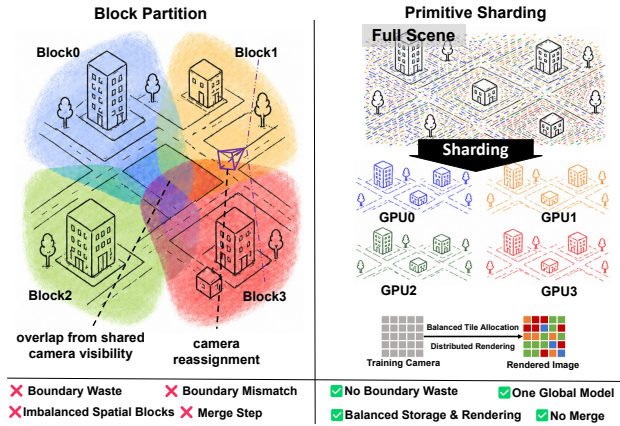


Figure 3. **Primitive sharding vs spatial block partitioning.** *Left:* block partitioning binds each GPU to a fixed scene region, so cameras near boundaries trigger overlap and reassignment. *Right:* BlitzGS shards one global Gaussian model across GPUs by index parity and distributes each render via balanced tile allocation, keeping both storage and rendering evenly spread.

3.3 Model Level Simplification

System level distribution balances per-iteration work across GPUs but does not reduce the global Gaussian count $|\mathcal{G}|$. Densification is necessary to reach final quality, yet by the end of it $|\mathcal{G}|$ is typically much larger than the scene strictly needs. A large $|\mathcal{G}|$ then slows every iteration regardless of how well the workload is sharded. BlitzGS therefore performs *permanent* population reduction at the model level. We score each Gaussian by its contribution density aggregated over the training views (defined formally in Eq. 3 below). This measure combines how often the primitive is rendered with how strongly it contributes per pixel when it does contribute. Computing this score over a city-scale population is too expensive to run every iteration, so we evaluate it in *scheduled simplification passes* rather than continuously. Figure 4 summarises one such pass.

Importance score. An importance-scoring pass is a single sweep over all V training views with an instrumented rasterizer that bypasses color shading. For each view v and each Gaussian g_i projected onto pixels in v , the rasterizer records the alpha-weight $w_{i,v}$ that g_i contributes summed across the pixels it touches, and the projected support area $a_{i,v}$, the number of pixels it touches. The pass aggregates these into a single per-Gaussian score

$$s_i = \sum_{v: a_{i,v} > 0} \frac{w_{i,v}}{a_{i,v} + \epsilon}, \quad s_i = 0 \text{ if no view covers } g_i, \quad (3)$$

where ϵ is a small constant for numerical stability. This is contribution *density* per pixel rather than total screen coverage. Area normalisation matters at city scale. Without it, large blurry Gaussians on aerial backgrounds dominate purely through pixel count, which are erroneously preserved by the simplifier instead of actually desired fine facade details. The score is recomputed from scratch in each importance-scoring pass; it is not updated during regular training iterations.

Scheduled simplification. We use two importance-scoring passes that apply complementary pruning rules. The first pass reduces the population by *stochastic* importance-weighted sampling without replacement: it draws a fixed fraction of the current set with sample probability proportional to s_i , so high-contribution primitives survive almost surely while a long tail is admitted with non-zero probability. The second pass applies a *deterministic* cumulative-mass cut that retains the smallest prefix of Gaussians whose summed score reaches a target fraction (we use 99%) of the total and prunes the rest. The first pass (early, at T_1) primarily safeguards quality, while the second pass (late, at T_2) primarily trims the final population. Each pass is followed by an index-parity redistribution that rebalances the survivors across shards.

Feedback into the training. The same dedicated sweep that produces s_i also yields two additional per-Gaussian quantities at no

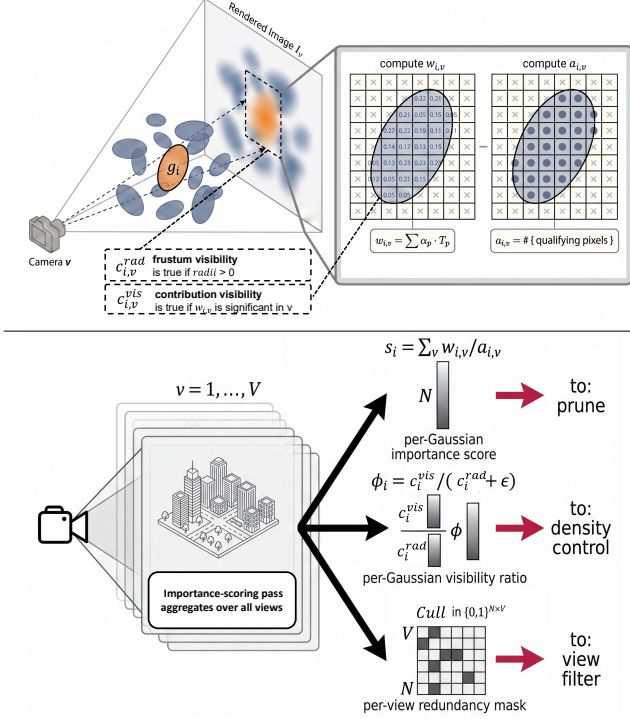


Figure 4. **Inside one importance-scoring pass.** For each training camera v (top), our rasterizer records two per-pixel cumulative quantities for every Gaussian g_i : the alpha-weight $w_{i,v} = \sum_p \alpha_p T_p$ and the qualifying-pixel count $a_{i,v}$. Two per-(Gaussian, camera) visibility bits are also derived: $c_{i,v}^{rad}$ (frustum visibility, radii > 0) and $c_{i,v}^{vis}$ (contribution visibility, $w_{i,v}$ in the per-view top-99% mass). Aggregating across all V views (bottom) yields three per-Gaussian feedback signals that share this one sweep: the importance score $s_i = \sum_v w_{i,v} / a_{i,v}$ used to prune; the visibility ratio $\phi_i = c_i^{vis} / (c_i^{rad} + \epsilon)$ that reweights density control; and the per-view redundancy mask $Cull \in \{0, 1\}^{N \times V}$ (the complement of c_i^{vis}) consumed by the view level filter.

extra rendering cost, which we feed back into both density control and view level filtering. For each Gaussian and each view, the rasterizer additionally records two visibility bits: $c_{i,v}^{rad}$ (frustum visibility, true when $\text{radii}_{i,v} > 0$) and $c_{i,v}^{vis}$ (contribution visibility, true when $w_{i,v}$ falls inside the per-view top-99% mass). Aggregating across views gives the counts $c_i^{rad} = \sum_v c_{i,v}^{rad}$ and $c_i^{vis} = \sum_v c_{i,v}^{vis}$, and the ratio $\phi_i = c_i^{vis} / (c_i^{rad} + \epsilon)$ measures how often g_i is genuinely contributing if it is visible. Whenever density control is active in a window that has access to a recent ϕ_i , the gradient-magnitude statistic that drives clone-and-split is reweighted by this factor. Because the scheduled passes leave a much smaller global population, this reweighting steers the remaining densification onto primitives that are consistently contributing across many cameras, so the simplified model still spends its capacity where it most affects view quality rather than diluting it across redundant clones. The same sweep also writes the bit-packed per-view redundancy matrix $Cull \in \{0, 1\}^{N \times V}$ consumed by the view level filter (Sec. 3.4). It is defined as the complement of contribution visibility ($Cull_{i,v} = 1 - c_{i,v}^{vis}$), so $Cull_{i,v} = 1$ flags Gaussians that fall outside the per-view top-99% mass. This design therefore plays three roles at once: it permanently shrinks the

population, redirects the remaining densification onto the highest-contribution primitives so the smaller model still meets the quality target, and selects which subset each camera renders. All three roles are driven by the same multi-view importance signal computed in one sweep.

3.4 View Level Filtering

The system level sharding distributes primitives across devices and the model level simplification trims the global set. At the view level, BlitzGS further trims the active set entering each render through two complementary filters: a *distance-based LOD gate* and an *importance-based per-view culling mask*.

Distance-based LOD gate. Each Gaussian carries an LOD label $\ell_i \in \{0, \dots, K-1\}$ attached at multi-resolution voxelisation of the SfM cloud [Ren et al. 2024]. The label is propagated through density control by a simple heritage rule: clone keeps the parent’s level, split increments by one. The level structure therefore remains a stable property of the model rather than a render-time-only mask. For a camera with centre c_o at training iteration t , the renderer estimates the finest level resolvable at distance d ,

$$L_o(d, t) = \text{clamp}(\lfloor \log_f(d_0/d) \rfloor, 0, L_{\max}(t)), \quad (4)$$

and keeps only Gaussians with equal or lower levels:

$$\mathcal{L}_v^{(m)}(t) = \{g_i \in \mathcal{G}^{(m)} : \ell_i \leq L_o(\| \mu_i - c_o \|, t)\}. \quad (5)$$

d_0 is a reference camera-to-scene distance computed from the training cameras at initialisation and held fixed, and $f = 2$ is the geometric ratio between consecutive LOD levels. $L_{\max}(t)$ unlocks levels coarse-to-fine on a geometric schedule so the LOD set’s ceiling tracks the population that has actually formed. The gate itself is disabled during the early density-control window so masked-out Gaussians do not lose densification credit. We fall back to the full shard whenever the predicted ratio $|\mathcal{L}_v^{(m)}(t)| / |\mathcal{G}^{(m)}|$ is close to one, so as to skip the gate when it would barely filter anything.

Importance-based per-view culling mask. The importance-scoring passes of Sec. 3.3 maintain, alongside the per-Gaussian score, a bit-packed per-view redundancy matrix $Cull \in \{0, 1\}^{N \times V}$ that flags, for every camera, the Gaussians whose contribution to that camera fell below the per-view top quantile in the most recent sweep. Whenever this mask is available, the main render consults the column corresponding to the current camera and skips the flagged Gaussians on top of the LOD gate, so the per-rank active set actually rasterized for view v becomes

$$\mathcal{A}_v^{(m)}(t) = \mathcal{L}_v^{(m)}(t) \setminus \{g_i : Cull_{i,v} = 1\}. \quad (6)$$

This filter and the LOD gate together apply two independent reductions to the per-camera active set: a geometric one driven by camera distance, and a contribution-based one driven by cross-view importance.

3.5 Supervision

For a mini-batch of B training cameras, each rank supervises only the image tiles it owns. The tile losses are reduced across ranks, and gradients propagate through both the rasterizer and the screen-space routing of Sec. 3.2. The photometric term is the standard RGB

reconstruction loss

$$\mathcal{L}_{\text{photo}} = \frac{1}{B} \sum_{b=1}^B (1 - \lambda) \|\hat{I}_b - I_b\|_1 + \lambda (1 - \text{SSIM}(\hat{I}_b, I_b)), \quad (7)$$

where $\lambda \in [0, 1]$ blends the L1 and SSIM terms. Following common practice in surface-aware 3DGS methods [Huang et al. 2024; Yu et al. 2024b], we add a regulariser that penalises the smallest scale axis of each Gaussian in the visible set \mathcal{V} to encourage surface-aligned primitives:

$$\mathcal{L} = \mathcal{L}_{\text{photo}} + \beta \mathcal{L}_{\text{scale}}, \quad \mathcal{L}_{\text{scale}} = \frac{1}{|\mathcal{V}|} \sum_{i \in \mathcal{V}} \min_j \sigma_{i,j}. \quad (8)$$

Here β weighs the scale regulariser and $\sigma_{i,j}$ is the standard deviation of g_i along its j -th principal axis of the covariance Σ_i . The acceleration in BlitzGS comes from controlling the active Gaussian workload rather than from auxiliary supervision; we therefore keep this objective lightweight and apply it consistently across all distributed tiles.

4 Experiments

4.1 Experimental Protocol

Datasets. We evaluate on the standard aerial benchmarks of large-scale 3DGS reconstruction: *Building* (1,940 train images) and *Rubble* (1,678) from Mill-19 [Turki et al. 2022], *Residence* (2,582) and *Sci-Art* (3,019) from UrbanScene3D [Lin et al. 2022], and the aerial split of *MatrixCity* (5,621) [Li et al. 2023a]. We follow the train/test camera splits released by Mega-NeRF [Turki et al. 2022] and UrbanScene3D, and the official aerial split of *MatrixCity*.

Baselines and metrics. We compare BlitzGS against representative large-scale 3DGS baselines: VastGaussian [Lin et al. 2024], CityGaussianV1 [Liu et al. 2024], CityGaussianV2 [Liu et al. 2025a], HUG [Su et al. 2025], Momentum-GS [Fan et al. 2025], and CityGS-X [Gao et al. 2025]. We report PSNR, SSIM, and LPIPS-VGG for novel-view synthesis on the held-out test cameras, together with training time.

Implementation details. All results are produced on 4×A6000 GPUs with batch size $B = 4$ unless otherwise stated. Density control runs every 500 steps from iteration 2,000 through 20,000, straddling the first importance-scoring pass at $T_1=15,000$; the LOD gate is disabled inside this window and engaged afterwards. The second importance-scoring pass is applied at $T_2=40,000$. After the first importance-scoring pass, density-control gradients are reweighted by the per-Gaussian visibility factor ϕ_i for the remainder of the density-control window. The loss weights are $\lambda=0.2$ and $\beta=10$. Training time is measured from launch to the final checkpoint. We refer the reader to our released code for the remaining implementation and hyperparameter details.

4.2 Quality-Speed Comparison

Table 1 shows that BlitzGS matches the rendering quality of recent large-scale 3DGS baselines across both real and synthetic aerial scenes while reducing training time by an order of magnitude. BlitzGS acwd hieves the highest PSNR on *Rubble* and *Residence*, sits essentially tied with the strongest baseline on *Building* and *Sci-Art*, and stays competitive on the synthetic *MatrixCity* scene.

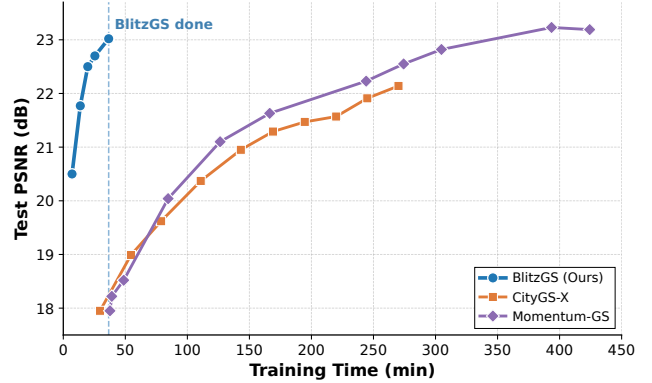


Figure 5. **Test PSNR over training time (*Building*)**. BlitzGS reaches a competitive PSNR within roughly 33 minutes (the steep curve ends at the vertical dashed line); CityGS-X and Momentum-GS continue to train for several more hours along noticeably shallower curves.

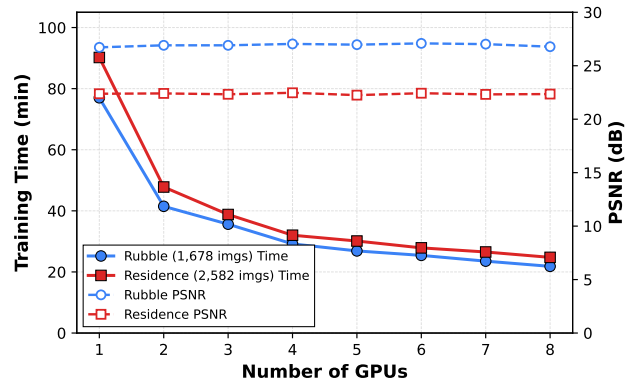


Figure 6. **Multi-GPU scaling across dataset sizes**. Color identifies the dataset (*Rubble*, 1,678 training images, blue; *Residence*, 2,582 training images, red); solid lines and filled markers are training time (left axis), dashed lines and hollow markers are PSNR (right axis). Training time drops monotonically on both datasets and the two curves are nearly parallel, reaching about 3.5–3.6× speedup at eight GPUs; PSNR stays within a tight per-scene band. Scaling is therefore largely independent of how many input images the scene contains. Measured on A800 80 GB GPUs because the $M=1$ configuration does not fit on a single 48 GB A6000.

Table 2 additionally reports the final Gaussian count and inference rendering speed.

To make the time-to-quality trade-off explicit, we additionally compare BlitzGS against CityGS-X and Momentum-GS on *Building*, on a per-checkpoint basis. We save a checkpoint at fixed iteration intervals during each method’s training and compute the held-out test PSNR from each checkpoint after all runs have finished. The resulting trajectories are plotted in Figure 5. The BlitzGS curve is short and steep, climbing to about 23 dB within roughly 36 minutes and ending there because training is over. CityGS-X and Momentum-GS keep training for 4–6 more hours along noticeably shallower curves; Momentum-GS catches up to a comparable PSNR by the end, while CityGS-X plateaus about 0.9 dB below BlitzGS. BlitzGS therefore matches or surpasses the eventual plateau of these baselines roughly an order of magnitude earlier in wall-clock time. This shape is consistent with of Sec. 3. Per-step compute is bounded by the system

Table 1. **Quality and reconstruction time on large-scale benchmarks.** We compare BlitzGS with baselines on standard novel-view synthesis metrics and training time. BlitzGS preserves competitive rendering quality while reducing city-scale training from hours to tens of minutes. Per metric and scene, the top three methods are highlighted with **red** / **orange** / **yellow** cell backgrounds for 1st / 2nd / 3rd respectively. Dashes (-) mark cells we could not reproduce because the corresponding baseline did not release a public checkpoint or training code for that scene.

Method	Building				Rubble				Residence				Sci-Art				MatrixCity			
	PSNR↑	SSIM↑	LPIPS↓	Time	PSNR↑	SSIM↑	LPIPS↓	Time	PSNR↑	SSIM↑	LPIPS↓	Time	PSNR↑	SSIM↑	LPIPS↓	Time	PSNR↑	SSIM↑	LPIPS↓	Time
VastGaussian [Lin et al. 2024]	21.80	0.728	0.225	5h48m	25.20	0.742	0.264	2h16m	21.01	0.699	0.261	5h05m	-	-	-	-	-	-	-	-
CityGaussianV1 [Liu et al. 2024]	21.55	0.778	0.246	8h07m	25.77	0.813	0.228	3h50m	22.00	0.813	0.211	8h33m	21.39	0.837	0.230	3h56m	27.46	0.865	0.204	12h17m
CityGaussianV2 [Liu et al. 2025a]	22.23	0.759	0.217	7h01m	24.58	0.767	0.252	4h16m	21.71	0.780	0.225	7h45m	21.49	0.811	0.238	10h35m	27.23	0.857	0.169	8h48m
Momentum-GS [Fan et al. 2025]	23.19	0.816	0.193	7h04m	25.91	0.829	0.197	5h03m	21.18	0.760	0.248	9h09m	20.75	0.794	0.266	6h27m	28.07	0.879	0.183	6h14m
HUG [Su et al. 2025]	22.35	0.792	0.228	5h16m	26.42	0.839	0.197	2h37m	22.33	0.813	0.207	6h31m	21.83	0.846	0.204	2h58m	28.02	0.883	0.142	10h04m
CityGS-X [Gao et al. 2025]	22.14	0.816	0.186	4h30m	24.92	0.831	0.199	6h03m	21.49	0.828	0.177	4h45m	23.31	0.872	0.178	3h14m	27.02	0.852	0.240	9h18m
BlitzGS (Ours)	23.02	0.798	0.234	36m35s	26.98	0.821	0.245	31m56s	22.50	0.829	0.210	35m08s	23.23	0.875	0.181	37m04s	27.02	0.856	0.224	1h16m

Table 2. **Component analysis of active workload control on Building (Mill-19).** Each row removes one component from the full BlitzGS configuration; all other settings are identical. The “w/o Pass-X pruning” variants skip only the population-reduction step inside the corresponding importance-scoring pass while keeping all of its signal computations (s_i , ϕ_i , and the *Cull* mask) untouched so the rest of the pipeline still consumes those signals.

Variant	PSNR↑	SSIM↑	LPIPS↓	FPS↑	it/s↑	Time↓	#GS↓
Full BlitzGS	23.02	0.798	0.234	194.0	45.6	36m35s	2.20M
w/o LOD gate	23.15	0.809	0.219	175.7	44.0	37m52s	2.89M
w/o importance scoring	23.05	0.807	0.217	148.2	35.7	47m46s	4.25M
w/o per-view importance mask	23.01	0.799	0.233	194.3	44.5	37m25s	2.24M
w/o ϕ_i density-control reweighting	22.86	0.799	0.232	185.8	49.2	33m51s	2.35M
w/o Pass-1 pruning	22.87	0.798	0.233	189.9	47.4	35m50s	2.29M
w/o Pass-2 pruning	22.96	0.802	0.227	162.2	38.4	37m50s	3.39M

level shard and view level active set, and population growth is constrained by the model level simplification–densification feedback. Each iteration therefore buys more PSNR per second, and the model reaches its target capacity in less training time.

4.3 Qualitative Results

Figure 7 compares BlitzGS against recent large-scale baselines on a held-out test view from each of eight scenes, with the ground truth alongside for reference. Across several views from each scene, BlitzGS recovers detail on par with the strongest baseline. The baselines reach good quality, but their optimization is still measured in hours; on the same multi-GPU hardware, BlitzGS brings training down to tens of minutes. Figure 8 highlights this advantage visually. When each baseline is stopped at the same training budget as BlitzGS (≈ 35 min), it remains visibly under-trained, while BlitzGS already produces clean reconstructions.

4.4 Ablation Study

We next examine how each level of workload control influences the speed-quality trade-off. Unless otherwise stated, all variants in this section use the default hyperparameters of Sec. 3 and toggle only the marked component.

Table 2 reports a leave-one-out ablation around the full BlitzGS configuration. The top three rows ablate workload interventions at the model and view levels. Removing the importance-scoring pass is the most damaging: the population nearly doubles (from 2.20M to 4.25M Gaussians), training takes about 30% longer, and inference FPS drops by about a quarter (to 148). Removing the LOD gate inflates the population by about 30% and drops FPS by 9%. The per-view importance mask has only a marginal effect once the LOD gate is in place, since the two filters overlap on Gaussians outside the

camera’s resolvable range. The remaining three rows isolate quality guardians inside the model level. Removing the ϕ_i reweighting costs 0.16 dB PSNR, confirming its role in concentrating densification onto view-contributory primitives. Removing Pass 1 pruning costs 0.15 dB while leaving inference FPS essentially unchanged, isolating the early pruning step as a quality contributor. Removing Pass 2 pruning leaves PSNR nearly unchanged but inflates the population by 54% and drops FPS to 162, identifying it as the long-tail trim.

The system level is ablated separately by sweeping the GPU count. Figure 6 shows that BlitzGS scales effectively across dataset sizes. The scaling study is run on A800 80 GB GPUs rather than the A6000 setup used elsewhere in this paper, because the $M=1$ configuration of these scenes does not fit in a single 48 GB A6000. On *Rubble* (1,678 training images) training time drops from 77 to 22 minutes as the GPU count grows from 1 to 8. On the larger *Residence* (2,582 training images) it drops from 90 to 25 minutes, with the two curves nearly parallel and reaching 3.5–3.6 \times speedup at eight GPUs. PSNR stays within a tight per-scene band on both datasets. The shape of the scaling curve is therefore largely independent of how many input images the scene contains, consistent with the system level workload model: per-step compute is bounded by the per-GPU shard rather than by the number of training views.

5 Conclusion

BlitzGS casts fast city-scale 3DGS reconstruction as an active workload-control problem and addresses it at three coupled levels. The *system level* shards Gaussians across GPUs by index parity and distributes each render step, avoiding the cross-block waste of spatial partitioning. The *model level* computes a multi-view importance signal in periodic importance-scoring passes that simultaneously prunes the population, reweights density-control gradients, and supplies a per-view culling mask. The *view level* filters each camera’s active set with a distance-based LOD gate and the importance mask. Trained only with an L1+SSIM photometric term and a scale regulariser, BlitzGS matches the rendering quality of recent large-scale baselines while bringing city-scale training from hours down to tens of minutes, and scales effectively from one to eight GPUs.

Several limitations remain. The LOD gate is a hard mask, so smooth fly-throughs can still reveal mild popping near level transitions; soft cross-fade alternatives would address this without giving up the per-Gaussian label. The importance-scoring schedule uses fixed checkpoints, which is reproducible but does not yet adapt to scene-specific densification dynamics. Finally, BlitzGS assumes the

global Gaussian set fits in the combined memory of the available GPUs. Scenes that exceed this aggregate capacity remain reachable by partition-based pipelines, which only need to hold one block at a time, whereas BlitzGS's non-spatial sharding does not directly extend to that regime.

References

- Jonathan T Barron, Ben Mildenhall, Dor Verbin, Pratul P Srinivasan, and Peter Hedman. 2022. Mip-nerf 360: Unbounded anti-aliased neural radiance fields. In *Proceedings of the IEEE/CVF conference on computer vision and pattern recognition*. 5470–5479.
- Danpeng Chen, Hai Li, Weicai Ye, Yifan Wang, Weijian Xie, Shangjin Zhai, Nan Wang, Haomin Liu, Hujun Bao, and Guofeng Zhang. 2024a. Pgsr: Planar-based gaussian splatting for efficient and high-fidelity surface reconstruction. *IEEE Transactions on Visualization and Computer Graphics* 31, 9 (2024), 6100–6111.
- Junyi Chen, Weicai Ye, Yifan Wang, Danpeng Chen, Di Huang, Wanli Ouyang, Guofeng Zhang, Yu Qiao, and Tong He. 2024b. Gigags: Scaling up planar-based 3d gaussians for large scene surface reconstruction. *arXiv preprint arXiv:2409.06685*.
- Yu Chen and Gim Hee Lee. 2024. Dogs: Distributed-oriented gaussian splatting for large-scale 3d reconstruction via gaussian consensus. *Advances in Neural Information Processing Systems* 37, 34487–34512.
- Kai Cheng, Xiaoxiao Long, Kaizhi Yang, Yao Yao, Wei Yin, Yuexin Ma, Wenping Wang, and Xuejin Chen. 2024. Gaussianpro: 3d gaussian splatting with progressive propagation. In *Forty-first International Conference on Machine Learning*.
- Jiadi Cui, Junming Cao, Fuqiang Zhao, Zhipeng He, Yifan Chen, Yuhui Zhong, Lan Xu, Yujiao Shi, Yingliang Zhang, and Jingyi Yu. 2024. Letsgo: Large-scale garage modeling and rendering via lidar-assisted gaussian primitives. 18 pages.
- Sankeerth Durvasula, Adrian Zhao, Fan Chen, Ruofan Liang, Pawan Kumar Sanjaya, and Nandita Vijaykumar. 2023. Distwar: Fast differentiable rendering on raster-based rendering pipelines.
- Jixuan Fan, Wanhua Li, Yifei Han, Tianru Dai, and Yansong Tang. 2025. Momentum-GS: Momentum Gaussian self-distillation for high-quality large scene reconstruction. In *Proceedings of the IEEE/CVF International Conference on Computer Vision*. 25250–25260.
- Zhiwen Fan, Wenyan Cong, Kairun Wen, Kevin Wang, Jian Zhang, Xinghao Ding, Danfei Xu, Boris Ivanovic, Marco Pavone, Georgios Pavlakos, et al. 2024a. Instantsplat: Sparse-view gaussian splatting in seconds.
- Zhiwen Fan, Kevin Wang, Kairun Wen, Zehao Zhu, Dejia Xu, and Zhangyang Wang. 2024b. Lightgaussian: Unbounded 3d gaussian compression with 15x reduction and 200+ fps. *Advances in neural information processing systems* 37, 140138–140158.
- Guangchi Fang and Bing Wang. 2024. Mini-splatting: Representing scenes with a constrained number of gaussians. In *European conference on computer vision*. Springer, 165–181.
- Guangchi Fang and Bing Wang. 2025. Efficient Scene Modeling Via Structure-Aware and Region-Prioritized 3D Gaussians.
- Guofeng Feng, Siyan Chen, Rong Fu, Zimu Liao, Yi Wang, Tao Liu, Boni Hu, Linning Xu, Zhilin Pei, Hengjie Li, et al. 2025. Flashgs: Efficient 3d gaussian splatting for large-scale and high-resolution rendering. In *Proceedings of the Computer Vision and Pattern Recognition Conference*. 26652–26662.
- Sara Fridovich-Keil, Alex Yu, Matthew Tancik, Qinhong Chen, Benjamin Recht, and Angjoo Kanazawa. 2022. Plenoxels: Radiance fields without neural networks. In *Proceedings of the IEEE/CVF conference on computer vision and pattern recognition*. 5501–5510.
- Yuanyuan Gao, Hao Li, Jiaqi Chen, Zhengyu Zou, Zhihang Zhong, Dingwen Zhang, Xiao Sun, and Junwei Han. 2025. Citygs-x: A scalable architecture for efficient and geometrically accurate large-scale scene reconstruction. In *Proceedings of the IEEE/CVF International Conference on Computer Vision*. 27187–27196.
- Antoine Guédon and Vincent Lepetit. 2024. Sugar: Surface-aligned gaussian splatting for efficient 3d mesh reconstruction and high-quality mesh rendering. In *Proceedings of the IEEE/CVF conference on computer vision and pattern recognition*. 5354–5363.
- Binbin Huang, Zehao Yu, Anpei Chen, Andreas Geiger, and Shenghua Gao. 2024. 2d gaussian splatting for geometrically accurate radiance fields. In *ACM SIGGRAPH 2024 conference papers*. 1–11.
- Bernhard Kerbl, Georgios Kopanas, Thomas Leimkühler, George Drettakis, et al. 2023. 3d gaussian splatting for real-time radiance field rendering. *ACM Trans. Graph.* 42, 4 (2023), 139–1.
- Bernhard Kerbl, Andreas Meuleman, Georgios Kopanas, Michael Wimmer, Alexandre Lanvin, and George Drettakis. 2024. A hierarchical 3d gaussian representation for real-time rendering of very large datasets. *ACM Transactions On Graphics (TOG)* 43, 4 (2024), 1–15.
- Shakiba Kheradmand, Daniel Rebain, Gopal Sharma, Weiwei Sun, Yang-Che Tseng, Hossam Isack, Abhishek Kar, Andrea Tagliasacchi, and Kwang Moo Yi. 2024. 3d gaussian splatting as markov chain monte carlo. *Advances in Neural Information Processing Systems* 37, 80965–80986.
- Bingling Li, Shengyi Chen, Luchao Wang, Kaimin Liao, Sijie Yan, and Yuanjun Xiong. 2024. Retinags: Scalable training for dense scene rendering with billion-scale 3d gaussians.
- Lingzhi Li, Zhen Shen, Zhongshu Wang, Li Shen, and Liefeng Bo. 2023b. Compressing volumetric radiance fields to 1 mb. In *Proceedings of the IEEE/CVF Conference on Computer Vision and Pattern Recognition*. 4222–4231.
- Yixuan Li, Lihan Jiang, Linning Xu, Yuanbo Xiangli, Zhenzhi Wang, Dahua Lin, and Bo Dai. 2023a. Matrixcity: A large-scale city dataset for city-scale neural rendering and beyond. In *Proceedings of the IEEE/CVF International Conference on Computer Vision*. 3205–3215.
- Jiaqi Lin, Zhihao Li, Xiao Tang, Jianzhuang Liu, Shiyong Liu, Jiayue Liu, Yangdi Lu, Xiaofei Wu, Songcen Xu, Youliang Yan, et al. 2024. Vastgaussian: Vast 3d gaussians for large scene reconstruction. In *Proceedings of the IEEE/CVF Conference on Computer Vision and Pattern Recognition*. 5166–5175.
- Liqliang Lin, Yilin Liu, Yue Hu, Xingguang Yan, Ke Xie, and Hui Huang. 2022. Capturing, reconstructing, and simulating: the urbanscene3d dataset. In *European Conference on Computer Vision*. Springer, 93–109.
- Yang Liu, Chuanchen Luo, Lue Fan, Naiyan Wang, Junran Peng, and Zhaoxiang Zhang. 2024. Citygaussian: Real-time high-quality large-scale scene rendering with gaussians. In *European Conference on Computer Vision*. Springer, 265–282.
- Yang Liu, Chuanchen Luo, Zhongkai Mao, Junran Peng, and Zhaoxiang Zhang. 2025a. Citygaussianv2: Efficient and geometrically accurate reconstruction for large-scale scenes. In *International Conference on Learning Representations*, Vol. 2025. 84324–84341.
- Yifei Liu, Zhihang Zhong, Yifan Zhan, Sheng Xu, and Xiao Sun. 2025b. Maskgaussian: Adaptive 3d gaussian representation from probabilistic masks. In *Proceedings of the Computer Vision and Pattern Recognition Conference*. 681–690.
- Tao Lu, Mulin Yu, Linning Xu, Yuanbo Xiangli, Limin Wang, Dahua Lin, and Bo Dai. 2024. Scaffold-gs: Structured 3d gaussians for view-adaptive rendering. In *Proceedings of the IEEE/CVF conference on computer vision and pattern recognition*. 20654–20664.
- Saswat Subhajoyti Mallick, Rahul Goel, Bernhard Kerbl, Markus Steinberger, Francisco Vicente Carrasco, and Fernando De La Torre. 2024. Taming 3dgs: High-quality radiance fields with limited resources. In *SIGGRAPH Asia 2024 Conference Papers*. 1–11.
- Ben Mildenhall, Pratul P Srinivasan, Matthew Tancik, Jonathan T Barron, Ravi Ramamoorthi, and Ren Ng. 2021. Nerf: Representing scenes as neural radiance fields for view synthesis. *Commun. ACM* 65, 1, 99–106.
- Thomas Müller, Alex Evans, Christoph Schied, and Alexander Keller. 2022. Instant neural graphics primitives with a multiresolution hash encoding. *ACM transactions on graphics (TOG)* 41, 4 (2022), 1–15.
- Lukas Radl, Michael Steiner, Mathias Parger, Alexander Weinrauch, Bernhard Kerbl, and Markus Steinberger. 2024. Stopthepop: Sorted gaussian splatting for view-consistent real-time rendering. *ACM Transactions on Graphics (TOG)* 43, 4 (2024), 1–17.
- Kerui Ren, Lihan Jiang, Tao Lu, Mulin Yu, Linning Xu, Zhangkai Ni, and Bo Dai. 2024. Octree-gs: Towards consistent real-time rendering with lod-structured 3d gaussians. *arXiv preprint arXiv:2403.17898* (2024).
- Shiwei Ren, Tianci Wen, Yongchun Fang, and Biao Lu. 2025. FastGS: Training 3D Gaussian Splatting in 100 Seconds.
- Samuel Rota Bulò, Lorenzo Porzi, and Peter Kotschieder. 2024. Revising densification in gaussian splatting. In *European Conference on Computer Vision*. Springer, 347–362.
- Mai Su, Zhongtao Wang, Huishan Au, Yilong Li, Xizhe Cao, Chengwei Pan, Yisong Chen, and Guoping Wang. 2025. HUG: Hierarchical Urban Gaussian Splatting with Block-Based Reconstruction for Large-Scale Aerial Scenes. In *Proceedings of the IEEE/CVF International Conference on Computer Vision*. 28839–28848.
- Matthew Tancik, Vincent Casser, Xinchen Yan, Sabeek Pradhan, Ben Mildenhall, Pratul P Srinivasan, Jonathan T Barron, and Henrik Kretzschmar. 2022. Block-nerf: Scalable large scene neural view synthesis. In *Proceedings of the IEEE/CVF conference on computer vision and pattern recognition*. 8248–8258.
- Haitthem Turki, Deva Ramanan, and Mahadev Satyanarayanan. 2022. Mega-nerf: Scalable construction of large-scale nerfs for virtual fly-throughs. In *Proceedings of the IEEE/CVF conference on computer vision and pattern recognition*. 12922–12931.
- Zhewei Yao, Amir Gholami, Daiyaan Arfeen, Richard Liaw, Joseph Gonzalez, Kurt Keutzer, and Michael Mahoney. 2018. Large batch size training of neural networks with adversarial training and second-order information.
- Zongxin Ye, Wenyu Li, Sidun Liu, Peng Qiao, and Yong Dou. 2024. Absgs: Recovering fine details in 3d gaussian splatting. In *Proceedings of the 32nd ACM international conference on multimedia*. 1053–1061.
- Zehao Yu, Anpei Chen, Binbin Huang, Torsten Sattler, and Andreas Geiger. 2024a. Mip-splatting: Alias-free 3d gaussian splatting. In *Proceedings of the IEEE/CVF conference on computer vision and pattern recognition*. 19447–19456.
- Zehao Yu, Torsten Sattler, and Andreas Geiger. 2024b. Gaussian opacity fields: Efficient adaptive surface reconstruction in unbounded scenes. *ACM Transactions on Graphics (ToG)* 43, 6 (2024), 1–13.
- Zheng Zhang, Wenbo Hu, Yixing Lao, Tong He, and Hengshuang Zhao. 2024. Pixel-gs: Density control with pixel-aware gradient for 3d gaussian splatting. In *European Conference on Computer Vision*. Springer, 326–342.

- Hexu Zhao, Haoyang Weng, Daohan Lu, Ang Li, Jinyang Li, Aurojit Panda, and Saining Xie. 2025. On scaling up 3d gaussian splatting training. In *International Conference on Learning Representations*, Vol. 2025. 35642–35661.
- MI Zhenxing and Dan Xu. 2022. Switch-nerf: Learning scene decomposition with mixture of experts for large-scale neural radiance fields. In *The Eleventh International Conference on Learning Representations*.

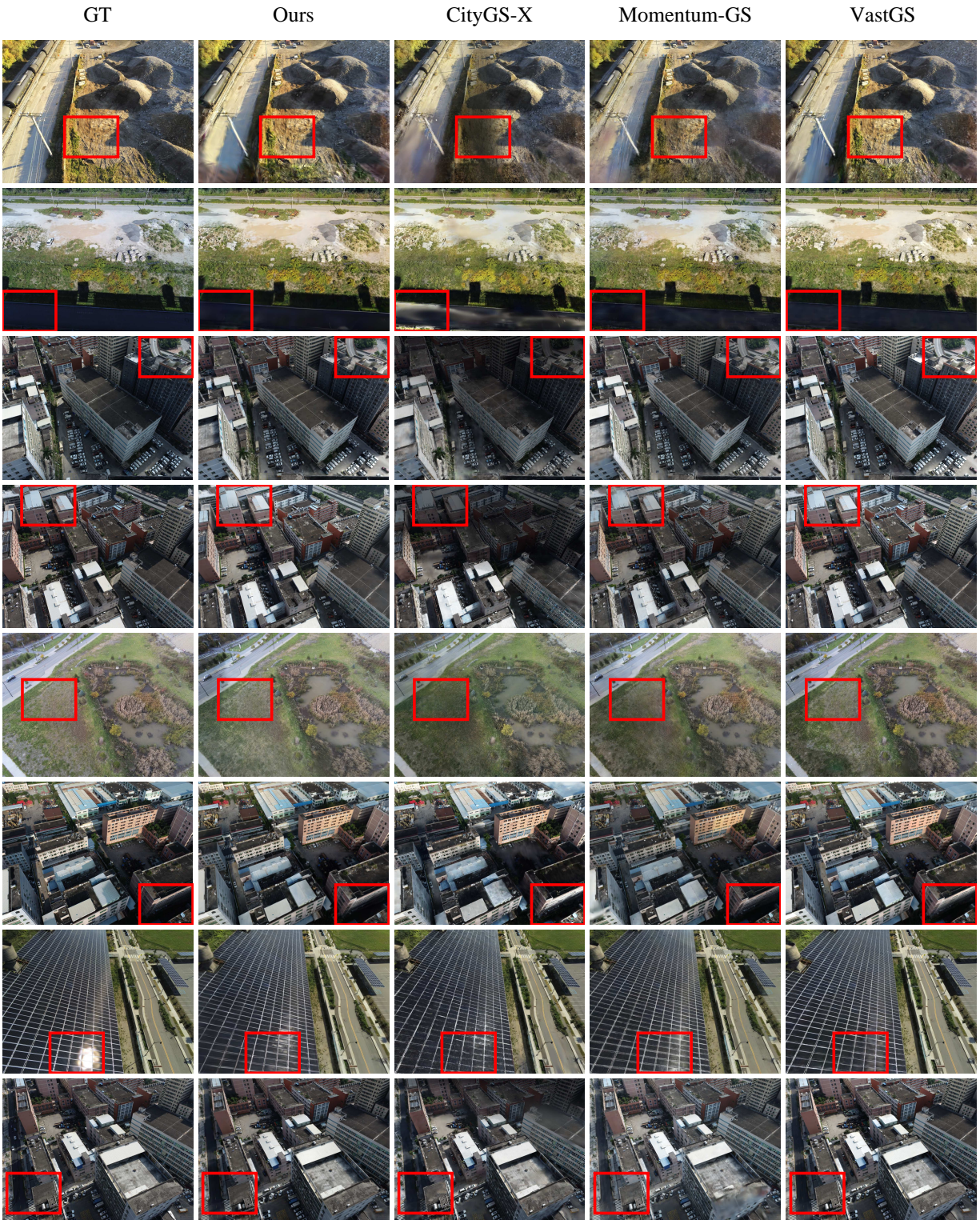


Figure 7. **Qualitative comparison on city-scale scenes.** Held-out test views from eight benchmark scenes; columns show GT, BlitzGS (Ours), CityGS-X, Momentum-GS, and VastGaussian. Red rectangles highlight close-ups where BlitzGS preserves detail comparable to or sharper than the baselines.

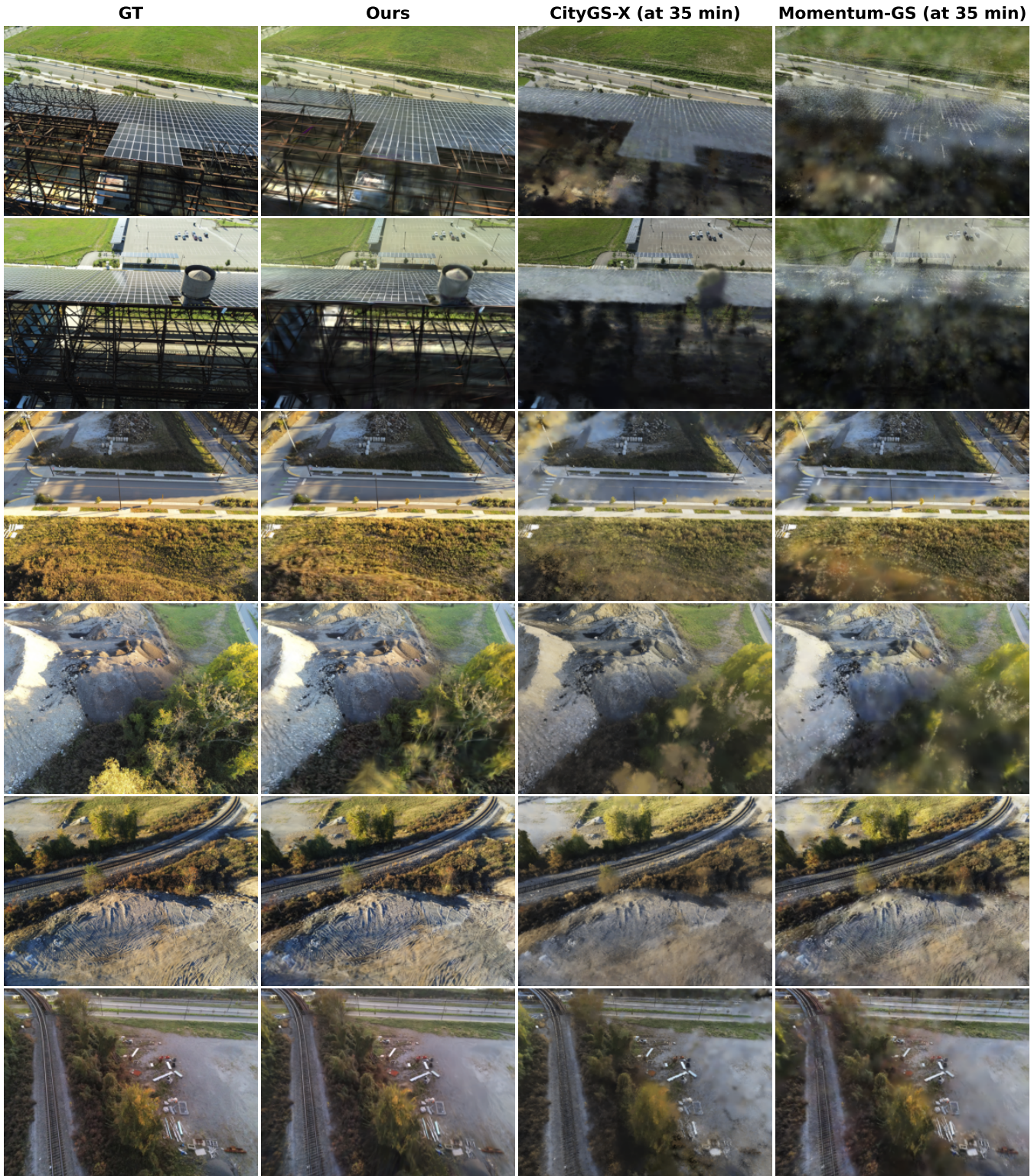


Figure 8. **Qualitative comparison at the same training budget (≈ 35 minutes).** Each baseline is shown at its checkpoint nearest BlitzGS's wall-clock budget; at this point CityGS-X and Momentum-GS are still under-trained while BlitzGS has finished.